JOURNAL OF CATALYSIS 127, 631–644 (1991)

Promoting Effects of Se on Rh/ZrO_2 Catalysis for Ethene Hydroformylation

Y. IZUMI, K. ASAKURA, AND Y. IWASAWA[1]

Department of Chemistry, Faculty of Science, The University of Tokyo, Hongo, Bunkyo-ku, Tokyo 113, Japan

Received May 16, 1990; revised September 11, 1990

The positive effects of Se added to Rh/ZrO_2 catalysts in ethene hydroformylation were studied from the viewpoints of promoter effects of electronegative atoms usually regarded as poisoning atoms as well as electronic interactions with both substrate metal and adsorbed species. Se-modified Rh/ZrO_2 catalysts prepared by the reactive deposition of $(CH_3)_2Se$ or coimpregnation method using SeO_2 were found to be active and selective for ethene hydroformylation. The Se addition promoted the formation of propanol rather than propanal, the propanol formation being increased more than 70 times at an optimumSe/Rh ratio. The propanoyl intermediates were observed at ca. 1770 $cm^{-1}$and converted reversibly to propionate species (bridge and bidentate) observed at 1425–1575 cm^{-1}. The ensemble of Se^{2-}/Rh was suggested to promote CO adsorption and the insertion of CO to ethyl species, where there is an electronic interaction between Se^{2-} and CO or propanoyl species. The isotope effects of D_2 and $^{13}C^{18}O$ showed the switchover of the rate-determining step for hydroformylation from the CO insertion on the Rh/ZrO_2 catalysts to the dissociative adsorption of H_2 on the $Se–Rh/ZrO_2$ catalysts. The role of Se is discussed in relation with the reaction mechanism.

INTRODUCTION

Promoting effects of the added second components on metal catalysis have extensively been studied from industrial points of view as well as from chemical interests (*1–3*). It has been demonstrated that the additive atoms which are electropositive to transition metals have the electron-donating properties to the surface metals and increase the catalytic activities (*4*). Numerous works on the effects of electropositive additives have been done particularly in CO hydrogenation on metal catalysts like Ni, Fe, Ru, and Rh (*2, 3*). Among group 8 metals, Rh most preferably produces C_2 oxygenates from CO/H_2 syngas. In Rh/SiO_2 systems, the additives such as Na, Mn, Fe, Zn, Ti, La, and Ce have been reported to enhance the reaction rates of CO hydrogenation or hydroformylation. Sodium promotes the formation of oxygenates in CO hydrogenation (*2*) or hydroformylation (*5*) on Rh/SiO_2 by ligand effect. Manganese can increase the rate of the formation of C_2 oxygenates in CO hydrogenation. In this case, the added manganese is known to be present in the form of $Mn^{2+}–O^{2-}$ on Rh metal surfaces (*6*). The very low-frequency peak at ca. 1715 cm^{-1} which is assignable to Rh–C–O–Mn species is observed with Mn–added Rh/SiO_2 catalysts (*7, 8*). However, the direct relation between the CO hydrogenation reactivity of the catalyst and this species has not been proven because it is difficult to follow the transformation from linear CO to the tilted CO species under *in situ* conditions by IR, and MnO layers on a Rh particle have the possibility of reconstructing as in SMSI suboxide migration (*7*). The iron additive promotes the formation of methanol and ethanol (*9*). Zinc has been reported to block bare metal sites of Rh/SiO_2 judging from the decrease of the relative ratio of bridged CO

0021-9517/91 $3.00

to linear CO with the addition of Zn, and also to interact with the oxygen atom of CO, leading to the enhancement of the CO insertion process (*10*). Ti, La, and Ce additions seem to be profoundly related to the SMSI phenomenon: these elements are distributed as oxides on Rh/SiO_2. TiO_x layers on Rh foil at TiO_x/surface Rh = 0.15 were active for methanation and the promotion mechanism has been referred to the $Rh–C–O–Ti^{3+}$ interaction at the edge of TiO_x layer (*11*). LaO_x on Rh/SiO_2 has been observed to promote the formation of methane, methanol, C_2–C_4 hydrocarbon, and C_2 oxygenates at La/surface Rh = 0.5 (*12*). Cerium also improves the selectivity to oxygenates (*13*). The low-frequency CO peaks at 1725 cm^{-1} observed with the La- or Ce-doped Rh/SiO_2 catalysts are similar to those for the case of Mn.

On the contrary, the addition of electronegative atoms may make metal atoms around the additive atoms positive. In this case, the mechanism for the creation of positive metal sites is different from that induced by site segregation of cationic additives. Electronegative additives may also have direct electronic interaction with the metal surface through chemical bonds. Back-donation of metal *d*-electrons to the CO $2\pi^*$ level is diminished by electron-withdrawing additives and adsorbed CO becomes harder to dissociate. The poisoning effects of S have been examined experimentally and theoretically. S poisons methanation and Boudouard reaction on Ni catalysts nonlinearly (*14*). MacLaren *et al.* (*15*) calculated the local density of states (LDOS) at Fermi level (E_f) of Rh(100) and Ni(100) surfaces by a MS–Xα method. They showed that S adatoms reduced LDOS at E_f resulting in poisoning to CO adsorption.They also estimated the area of the ligand (electronic) effect of S to be <5 Å laterally at surface. Feibelman and Hamann (*16*) have also reported similar results by surface-linearized-augmented-plane-wave (SLAPW) calculations. CO adsorption sites on S-modified Rh(111) and Ni(111) can be classified by the distance from threefold S adatoms: nearest sites M_A, far sites M_B, and remote sites M_C (*17*). The MS–Xα calculation suggests that M_B sites can promote CO adsorption to a small extent. This causes us to expect that Se, which has an electronegativity of 2.4 (similar to 2.5 for S), may have a positive effect on CO adsorption at the Rh surface and hence CO insertion. Furthermore, Se has been found to act as a good catalyst for liquid phase carbonylations, suggesting that the Se atom can interact with and activate CO (*18, 19*).

Thus we have examined the catalytic effect of electronegative Se additive on Rh/ZrO_2 in ethene hydroformylation (*20*). In this article, the promoting effects of Se on the activity and selectivity of Rh/ZrO_2 catalysts for ethene hydroformylation are reported. The interactions of Se with CO and reaction intermediates and the catalytic reaction mechanism are also discussed by kinetics, the tracer method, FT–IR, XPS, and temperature-programmed desorption (TPD).

EXPERIMENTAL

We prepared two different types of Se-modified Rh/ZrO_2 catalysts. Impregnated Rh/ZrO_2 catalysts were prepared by the usual impregnation method using aqueous solution of $Rh(NO_3)_3$ (Soekawa Co., Ltd.), followed by calcination at 673 K in air. ZrO_2 was obtained commercially (surface area, 12 $m^2\ g^{-1}$; Soekawa Co., Ltd.). Rh loading was 1 or 3 wt% as Rh/ZrO_2. The sample was reduced with H_2 at 673 K for 1 h. The Rh/ZrO_2 sample was preadsorbed with H_2 at a full coverage at 295 K and interacted with 0.025–0.12 kPa of $(CH_3)_2Se$ (Toyo Stauffer Chemical Co.) at 373 K for 30 min. The Se-modified catalyst was further treated with H_2 at 373 K for 30 min to remove weakly physisorbed $(CH_3)_2Se$. The Se-promoted Rh/ZrO_2 catalysts thus obtained are denoted as catalysts (**1**).

ZrO_2 was also coimpregnated with $Rh(NO_3)_3$ and SeO_2 (Tri Chemical Co., Ltd.) in aqueous solution, followed by calcination

at 673 K in air. The sample was reduced with H_2 at 673 K for 1 h. The catalysts thus obtained are denoted as catalysts(2).

The Se content of the catalysts was varied in the range of Se/Rh from 0.01 to 0.17. The amount of Se contained in each catalyst was determined by X-ray fluorescence. Se in the catalysts was not lost during the course of calcination, reduction, and hydroformylation. Ethene hydroformylation was carried out in the temperature range 393–473 K in a closed circulating system (dead volume, 119 cm^3) with a U-shaped liquid N_2-acetone trap (179 K). The reaction products were analyzed by gas chromatography using a 2-m column of VZ-10 at 353 K for ethene and ethane and a 4-m column of DOS at 353 K for propanal and propanol.

IR spectra were measured under *in situ* reaction conditions by FT-IR spectrometery (JASCO FT/IR-7000). A total of 0.03 g of the sample was pressed into a self-supporting disk which was placed in an IR cell with two NaCl windows which were combined with a closed circulating system. The spectra for adsorbed species were recorded by subtracting the gas phase spectra.

XPS spectra for Se $3d_{5/2}$ and Rh $3d_{5/2}$ and $3d_{3/2}$ were recorded on a Shimadzu ESCA750 spectrometer. The samples were transferred into the XPS chamber by a glove-box technique without contacting air. EXAFS spectra were measured at BL-10B of the Photon Factory in the National Laboratory for High Energy Physics (KEK-PF, Proposal No. 87-013). The EXAFS analysis was carried out using the theoretical phase shift and amplitude functions.

RESULTS

Surface Modification by $(CH_3)_2Se$

The reactivity of $(CH_3)_2Se$ with ZrO_2 or Rh/ZrO_2 is shown in Fig. 1. A total of 0.47 kPa of $(CH_3)_2Se$ was admitted onto the ZrO_2 surface at 373 K. The sample was heated at the rate of 4 K min^{-1} during TPD chromatography. Both methane and CO were evolved in the temperature range 573–723 K as shown in Fig. 1a. Methane formation

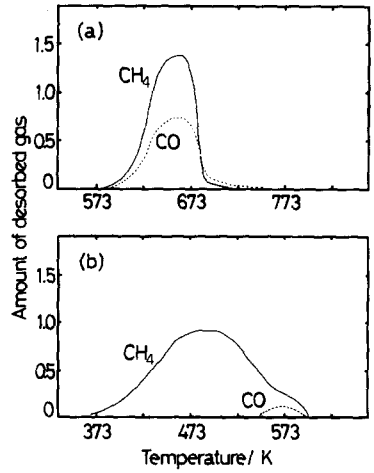

FIG. 1. TPD spectra of $(CH_3)_2Se$ on ZrO_2 (a) and Rh/ZrO_2 (b); 0.47 kPa of $(CH_3)_2Se$ was introduced in the circulating line and sampled to GC after trapping physisorbed $(CH_3)_2Se$ by liquid N_2 in the process of elevating the temperature by 4 K min^{-1}. Catalyst, 1.3 g; (a) desorbed CH_4 2.6×10^{-5} mol, CO 1.7×10^{-5} mol; (b) desorbed CH_4 4.3×10^{-5} mol.

indicates the reaction of $(CH_3)_2Se$ with OH groups at the ZrO_2 surface. CO may be formed by the oxidation of $(CH_3)_2Se$ with surface oxygen at ZrO_2. The molar amounts of methane and CO desorbed were twice that of the adsorbed $(CH_3)_2Se$, indicating that the reaction at the ZrO_2 surface occurs at temperatures higher than 573 K. On the contrary, when $(CH_3)_2Se$ was interacted with the Rh/ZrO_2 surface preadsorbed with H_2 (Fig. 1b, methane evolution started at 373 K and CO evolution was very low. The amount of desorbed CH_4 per adsorbed $(CH_3)_2Se$ equaled unity. These results mean that $(CH_3)_2Se$ preferentially reacted with hydrogen atoms adsorbed at the Rh metal surface to form CH_4 at 373 K rather than the surface OH groups of ZrO_2 (*21*) and the remaining $(CH_3)_2Se$ species completely reacted with the adsorbed hydrogen atoms before 573 K to leave $Se–CH_3$ species at the Rh surface. Thus Se atoms may modify the Rh surface selectively without their deposits on ZrO_2 surfaces.

The amount of the doped Se before and

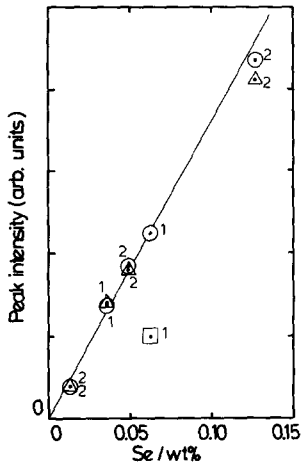

FIG. 2. X-ray fluorescence peak intensity vs the amount of Se supported on Rh/ZrO_2; ○, before hydroformylation; △, after hydroformylation, □, after H_2 treatment at 573 K; 1, catalyst (**1**); 2, catalyst (**2**).

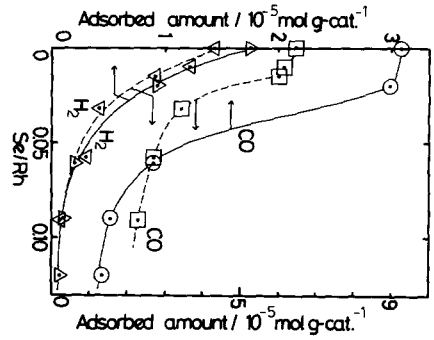

FIG. 3. The variation of the amounts of H_2 and CO adsorbed with the amount of Se contained in the catalysts (**2**); (———) Rh 1 wt%; (— — —) Rh 3 wt%.

after the hydroformylation reaction at 423 K for 5 h was determined by X-ray fluorescence. Figure 2 shows the linear relationship between the peak intensities of X-ray fluorescence and the amounts of Se doped in catalysts (**1**) and catalysts (**2**). It is suggested that Se was not lost during the reaction at 423 K by the fact that the peak intensity for Se contained in the catalysis did not change by the catalytic performance as shown in Fig. 2. However, the peak intensity decreased to almost half by reaction with H_2 at 573 K.

H_2 and CO Adsorptions

H_2 and CO adsorptions on the catalysts (**1**) and (**2**) were volumetrically measured. H/Rh values were 0.36 and 0.29 for Rh/ZrO_2 (1 wt%) and Rh/ZrO_2 (3 wt%), respectively. The TEM photographs showed the averaged particle sizes of 36 and 45 Å for the catalysts which are compatible with the H/Rh values. The TEM images of the Se-doped catalysts (**1**) and (**2**) did not essentially change as compared with those of the undoped catalysts. The notation "Se/Rh" means the ratio of the number of total Se atoms to that of total Rh atoms, while the notation "Se/surf. Rh" means the number of Se atoms per the surface Rh atoms which are the number of surface Rh atoms determined by H/Rh values.

As typically shown in Fig. 3, the amount of H_2 adsorbed at 293 K decreased monotonically almost zero as the Se quantity increased. In contrast, the amount of CO adsorption remained almost unchanged or reduced much more slowly with an increase of Se/Rh up to 0.02. At the larger amounts of Se the CO adsorption decreased, but it was possible to adsorb even at Se/Rh > 0.10, where the H_2 adsorption was nearly zero as shown in Fig. 3. These results suggest that Se atoms at the Rh surface can interact with adsorbed CO.

The IR peaks for CO adsorbed on the catalysts (**2**) are listed in Table 1, where linear (2068 cm^{-1}), bridge (ca. 1900 cm^{-1},

TABLE 1

IR Peaks (cm^{-1}) for Adsorbed CO on Catalysts (**2**)

Catalyst Se/Rh	Rh/ZrO_2 (0)	Se–/Rh/ZrO_2 (0.019)	Se–Rh/ZrO_2
Linear	2068(s)	2068(s)	2068(s)
Bridge	1900(w,br)	1908(w,br)	1922(w,br)
Twin	2094(m)	n.o.	n.o.
	2040(m)	n.o.	n.o.

Note. CO was adsorbed at 293 K; n.o., not observed.

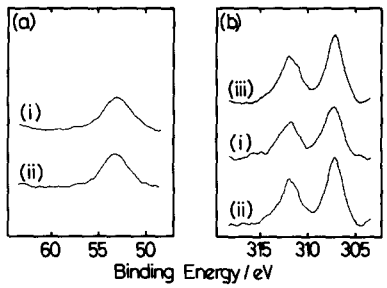

FIG. 4. XPS spectra of Se $3d_{5/2}$ (a) and Rh $3d_{3/2}$, $3d_{5/2}$ (b) for Rh/ZrO_2 catalysts (iii) and Se-doped Rh/ZrO_2 catalysts (**3**) (Se/Rh = 0.012) (i,ii) before and after ethene hydroformylation at 453 K; (i) before hydroformylation; (ii) after hydroformylation.

broad), and twin (2094 and 2040 cm^{-1}) CO peaks are distinguishable. The twin CO peaks, in addition to linear and bridge peaks, were observed with the Rh/ZrO_2 sample, whereas no twin CO peaks were observed on the Se-modified surfaces, suggesting that Se preferentially blocked the twin sites on Rh metal surfaces of the Rh/ZrO_2 catalyst.

XPS Measurements

XPS binding energies for the Se $3d_{5/2}$ level and Rh $3d_{3/2}$ and $3d_{5/2}$ levels were measured before and after ethene hydroformylation at 453 K as shown in Fig. 4. The Se $3d_{5/2}$ binding energy for the catalyst (**2**) with Se/Rh = 0.012 before the reaction was determined to be 53.2 eV. The value was almost the same also with the sample after the reaction as shown in Fig. 4. Again, the binding energy was independent of the Se content in the catalysts in the range of Se/Rh = 0.01–0.13. These results reveal that the oxidation state of Se is −2 for all the catalysts (**2**) employed in the present study and Se atoms are situated in a −2 state during the catalytic reaction. The XPS peaks for Rh $3d_{3/2}$ and $3d_{5/2}$ were always observed at 311.8 ± 0.1 and 307.2 ± 0.1 eV, respectively, as shown in Fig. 4. The values are almost the same as those for undoped Rh/ZrO_2 and correspond to the binding energies for metallic Rh. No shoulder on the higher binding energy side of the metallic Rh peaks was observed with the sample of Se/Rh = 0.01–0.13, suggesting no presence of positive Rh atoms at the surface. The similar binding energies for Se and Rh $3d$ levels were observed with the catalysts (**1**) prepared by using $(CH_3)Se$, showing the oxidation states of Se^{2-} and Rh^0.

EXAFS Measurements

It was not possible to observe the bonding between Rh and Se for the present catalysts because of the large particle size of Rh metal. In turn, no observation of Rh–Se bonds may exclude the possibility of the atomic distribution of Se in the Rh bulk. In order to examine whether or not Se^{2-} can bind with the Rh atom, we prepared Se–Rh/ZrO_2 catalysts by using $Rh_6(CO)_{16}$ and $(CH_3)_2Se$ and measured the EXAFS spectra of the obtained catalyst under air-free conditions. The EXAFS analysis showed the Rh–Se bonds at 2.41 Å.

Catalytic Ethene Hydroformylation

Ethane, propanal, and propanol were formed in ethene hydroformylation on the catalyst (**1**) (Se/Rh = 0.066) at 453 K in a closed circulating system. At the initial period of the reaction on the fresh catalyst (**1**), acataldehyde was also produced by the reaction between CO and the remaining methyl group derived from $(CH_3)_2Se$, but its formation ceased within 20 min and was not observed in the second run. When the amount of Se added in the catalyst (**1**) increased, the formations of ethane and propanal were drastically suppressed, whereas the reaction rate of propanol formation increased and showed the maximum value around Se/Rh = 0.07 as shown in Fig. 5. The hydroformylation reaction did not significantly proceed on the catalysts with Se/Rh > 0.10.

The turnover frequencies (TOF) of the reactions on the Se–Rh/ZrO_2 catalysts (**1**) as a function of Se content were shown in Fig. 6. The TOF is defined as the initial reaction rate divided by the amount of hydrogen atoms adsorbed on the catalysts.

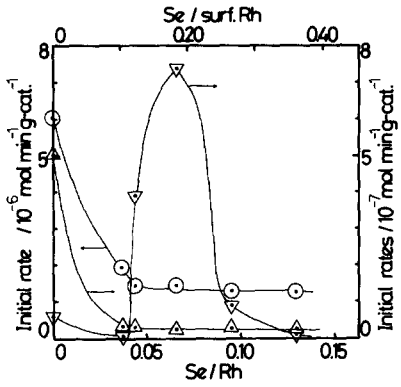

FIG. 5. Catalytic activities of the Se-modified catalysts (**1**) for ethene hydroformylation as a function of Se content; react. temp., 453 K; total pressure, 40.0 kPa; $C_2H_4:CO:H_2 = 1:1:1$, Rh 1 wt% ○, ethane; △, propanal; ▽, propanol.

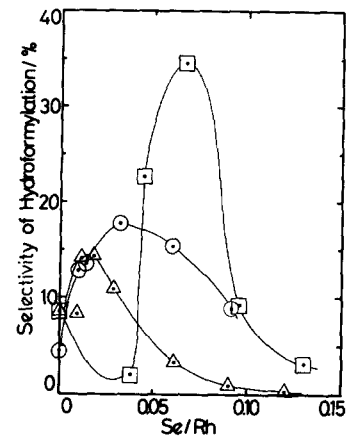

FIG. 7. The selectivities of ethene hydroformylation on Se–Rh/ZrO_2 catalysts (**1**) and (**3**) as a function of Se content; □, catalyst (**1**) (Rh 1 wt%); △, catalysts (**2**) (1 wt%); ○, catalysts (**2**) (3 wt%); react. temp., 453 K.

The TOF for propanol formation remarkably increased at the optimum Se/Rh ratio. Note that the ethane formation was enhanced in the higher region of the Se content. As a result, the TOF for propanol formation on the catalyst (**1**) modified with Se of the optimum quantity was larger by a factor of 70 than the TOF for the Rh/ZrO_2 catalyst without Se.

The selectivities of ethene hydroformylation on the catalysts (**1**) were plotted against the Se content as shown in Fig. 7.

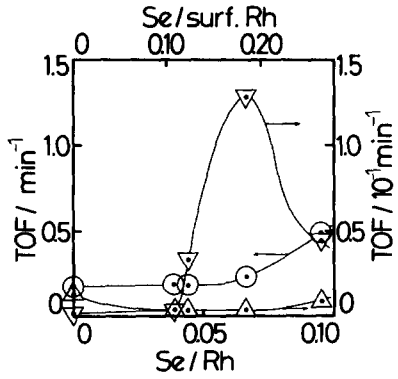

FIG. 6. Turnover frequencies of ethene hydroformylation on the Se-modified catalysts (**1**) as a function of Se content; TOF is defined as the initial rate devided by exposed Rh judged by H_2 adsorption; react. temp., 453 K; total pressure, 40.0 kPa; $C_2H_4:CO:H_2 = 1:1:1$, Rh 1 wt%; ○, ethane; △, propanal; ▽, propanol.

The selectivity of the catalyst with Se/Rh = 0.066 was more than four times higher than that of the undoped catalyst.

The catalytic performance on the catalysts (**2**) is shown in Fig. 8. The hydroformylation rates did not drastically increase by changing the Se quantity as compared with the case of the catalysts (**1**). However,

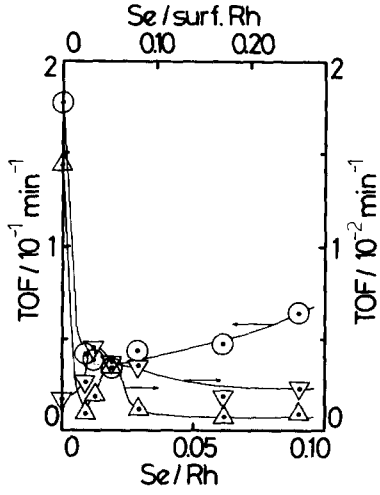

FIG. 8. Turnover frequencies of ethene hydroformylation on the Se-modified catalysts (**2**) as a function of Se content; TOF is defined as the initial rate devided by exposed Rh judged by H_2 adsorption; react. temp., 453 K; total pressure, 40.0 kPa; $C_2H_4:CO:H_2 = 1:1:1$, Rh 1 wt%; ○, ethane; △, propanal; ▽, propanol.

TABLE 2

Activation Energies for Ethene Hydroformylation on Rh/ZrO_2, $Se-Rh/ZrO_2$, and Rh/SiO_2 Catalysts

	Activation energies (kJ mol^{-1})			
	Ethane	Propanal	Propanol	C_3-oxo
Rh/ZrO_2	60	22	30	27
$Se-Rh/ZrO_2(0.019)$	53	0.9	36	17
Rh/SiO_2	56	89	—	89

Note. $C_2H_4 : CO : H_2$ = 13.3 : 13.3 : 13.3 kPa; temperature range, 393–473 K.

the optimum amount of Se added for the formation of the hydroformylation products was observed.

The selectivities of hydroformylation on the catalysts (**2**) with the Rh loadings of 1 and 3 wt% are shown in Fig. 7. The curves had the maximums at Se/Rh = 0.019 (Se/surf. Rh = 0.052) for Rh 1 wt% and at Se/Rh = 0.032 (Se/surf. Rh = 0.11) for Rh 3 wt%.

The activation energies for the formations of ethane, propanal, and propanol in ethene hydroformylation are listed in Table 2. The activation energy for propanal formation was much lower on the Rh/ZrO_2 catalyst than on the Rh/SiO_2 catalyst. The apparent activation energy for propanal formation on the $Se-Rh/ZrO_2$ catalyst was extremely small. On $Se-Rh/ZrO_2$ catalysts, the propanal yield is determined by a balance of two rates of the propanoyl-to-propanal step and the propanal-to-propanol step. Se was suggested to affect both rates with different temperature dependencies and particularly to promote propanol formation, resulting in the small activation energy, as described hereinafter.

In Situ Observation of Surface Species by FT–IR

The behavior of the surface species on the catalysts during ethene hydroformylation was followed by FT–IR. Figure 9 shows the spectra after ethene hydroformylation on the Rh/ZrO_2 catalysts (**2**) having Se/Rh = 0, 0.019, and 0.061 for 1 h. Besides the linear CO peaks at 2040–2048 cm^{-1}, the peaks around 1770 cm^{-1} and in the region 1400–1600 cm^{-1} were observed in Fig. 9. The peak intensity around 1770 cm^{-1} increased as the Se content increased from 0 to 0.019, but decreased by the further addition of Se to the catalyst. When CO was admitted to the catalyst surfaces at 453 K, no peak around 1770 cm^{-1} was observed. Its peak appeared only under reaction conditions. These results indicate that the peak around 1770 cm^{-1} is not referred to molecular CO-derived adspecies. In order to assign the peak around 1770 cm^{-1}, propanal was adsorbed at 190 K in the presence of H_2, showing a peak at 1710 cm^{-1}. The peak frequency is similar to 1728 cm^{-1} for liquid propanal and the peak at 1710 cm^{-1} is assigned to the molecularly adsorbed propanal. The peak around 1770 cm^{-1} is also suggested not to be referred to adsorbed propanal as a product in ethene hydroformylation. When the adsorbed propanal was heated to 453 K, the same peak as that around 1770 cm^{-1} in Fig. 9 appeared. Upon the reaction of D_2 with the species giving the peak around 1770 cm^{-1}, propanal was produced, where D atoms were incorporated to aldehydic hydrogen. These results suggest the peak is assignable to propanoyl species.

Two peaks of ca. 1575 and ca. 1425 cm^{-1} may be assigned to ν_{as} and ν_s of bridge-type

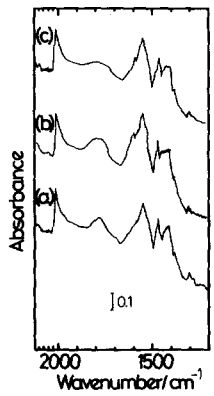

FIG. 9. *In situ* FT–IR spectra after ethene hydroformylation on the catalysts (**2**) for 1 h at 453 K; Rh 1 wt%; (a) Se/Rh = 0; (b) Se/Rh = 0.019; (c) Se/Rh = 0.061; total pressure, 40.0 kPa; $C_2H_4 : CO : H_2$ = 1 : 1 : 1.

TABLE 3

Assignments of IR Peaks Observed during Ethene Hydroformylation on Catalysts (2) at 453 K

Catalyst Se/Rh	Rh/ZrO_2 (0)	$Se—Rh/ZrO_2$ (0.019)	Se–Rh/ZrO (0.061)
Linear CO	2048	2044	2040
Propanoyl	1776	1770	1766
Propionate (bidentate)	1540	1543	1549
	1476	1473	1475
Propionate (bridge)	1576	1575	1573
	1426	1425	1423

propionate species, respectively, and the peaks at ca. 1545 and ca. 1475 cm^{-1} to ν_{as} and ν_s of bidentate-type propionate species, respectively, judging from the peak frequencies and the peak separation. The peaks at the similar frequencies were observed by introducing propionic acid into the Rh/ZrO_2 catalyst at 453 K. When propanoyl species were formed from propanal and kept at 453 K, a similar spectrum in the region 1400–1600 cm^{-1} appeared. The Boudouard reaction on any $Se–Rh/ZrO_2$ catalysts did not take place at 453 K, leaving no oxygen atoms on the Rh metal surface. These results suggest that under the reaction conditions propionate species are produced from propanoyl by reaction with surface oxygen atoms of ZrO_2 support. The peak assignments are given in Table 3. We checked the linearity between IR peak intensities and concentrations of adspecies by determination of the amount of species desorbed from the surface monitored by IR.

The peaks of propanoyl and propionate species increased in a similar manner during ethene hydroformylation at the total pressure of 40.0 kPa ($C_2H_4 : CO : H_2 = 1 : 1 : 1$) and 453 K, and saturated at 10, 30, and 50 min of passed reaction time for the catalysts (2) with Se/Rh = 0.019 and 0.061, respecspectively. The reactions on the catalysts (1) and the catalysts (2) without Se steadily proceeded from the beginning of reaction, whereas certain induction times of ca. 30 and ca. 50 min were observed for catalysts (2) with Se/Rh = 0.019 and 0.061, respectively. The rates of the formation of propanoyl and propionate species under the catalytic reaction conditions were determined by following the increase of their IR peaks as given in Table 4.

The rate of the conversion of propanoyl to propionate species was determined as follows. Propanal was admitted to the catalyst surface at 453 K to form propanoyl corresponding to the amount of propanoyl species in the steady state of reaction. The decrease in the propanoyl peak and the increase in the propionate peaks were followed by IR. The rates of elementary steps on the three catalysts are given in Table 4.

In order to determine the rate of the conversion of propionate to propanoyl, only the propionate species were produced as follows. The temperature-programmed desorption measurement in the presence of H_2 revealed that it is possible to desorb propanoyl and leave only propionate at the catalyst surfaces as shown in Fig. 10. Hence, the gas phase in the catalytic system under the hydroformylation conditions at 453 K was evacuated and heated up to the suitable temperatures around 480 K depending on the catalysts in the presence of H_2, followed by evacuation. The catalysts were cooled down to 453 K in a few seconds and the decrease of propionate and the increase of propanoyl were followed by IR. Small portions of the formed propanoyl were further decomposed to reaction gas. The initial rate of the propionate to propanoyl step is given in Table 4.

TABLE 4

Reaction Rates of Each Step on the Rh/ZrO_2 Catalysts (2) at 453 K

Reaction step	Rate (10^{-7} mol min^{-1} $g\text{-}cat^{-1}$)		
	Se/Rh		
	0	0.019	0.061
$C_2H_4 + CO + H_2 \rightarrow C_2H_5CO(a) + C_2H_5COO(a)$	5.5	1.3	0.7
$C_2H_5CO(a) \rightarrow C_2H_5COO(a)$	8.4	8.8	8.5
$C_2H_5COO(a) \rightarrow C_2H_5CO(a)$	1.4	2.6	2.5
$C_2H_5CO(a) + H_2 \rightarrow C_2H_5CHO + C_3H_7OH$[a]	7.5	1.7	0.8
Catalytic ethene hydroformylation	5.9	1.2	0.73

[a] In the presence of CO similar to the catalytic hydroformylation reaction.

After the ethene hydroformylation reaction was conducted for 10–50 min and the equilibrium between propanoyl and propionate species was attained, the gas phase was evacuated and H_2 was introduced into the system. The decrease in the peaks of propanoyl and propionate was observed by IR. The rate of the reaction of propanoyl with H_2 was determined from the initial rate of the decrease in the propanoyl peak, taking into account the contribution of propionate species. The values are given in Table 4.

Temperature-Programmed Desorption of Surface Species

The temperature-programmed desorption of the surface species formed during catalytic ethene hydroformylation is shown in Fig. 10. The temperature of the catalyst (disk) was linearly raised from 293 to 673 K at a heating rate of 4 K min^{-1} and the intensity changes of propanoyl and propionate peaks were measured by FT–IR. The desorption of propanoyl species on the undoped Rh/ZrO_2 catalyst was observed at the lowest temperature. The desorption temperature increased with an increase of Se content as shown in Fig. 10a. This tendency was similar also in the case of propionate species as shown in Fig. 10b. The desorption temperature of propionate species was higher than that of propanoyl species on each catalyst, suggesting that the former species is more stable than the latter.

The TPD spectra for the products desorbed from the propanoyl and propionate species was taken by gas chromatography (GC) in the presence of H_2 under experimental conditions similar to those in Fig. 10. The products were propanal, ethene, and ethane. The desorption temperature for propanal was found to coincide with that for the propanoyl species as shown in Fig. 11a and the desorption temperature for ethene and ethane was the same as that for the propionate species as shown in Fig. 11b. This coincidence was observed with all the catalysts, suggesting that the propanoyl species re-

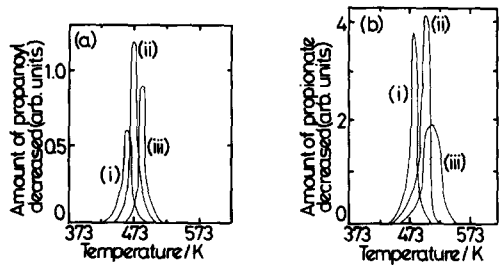

FIG. 10. TPD spectra in the presence of H_2 for the propanoyl species(a) and the propionate species (b) produced during ethene hydroformylation on the catalysts (2) observed by FT–IR; heating rate, 4 K min^{-1}; H_2; 13.3 kPa; (i) Se/Rh = 0; (ii) Se/Rh = 0.019; (iii) Se/Rh = 0.061.

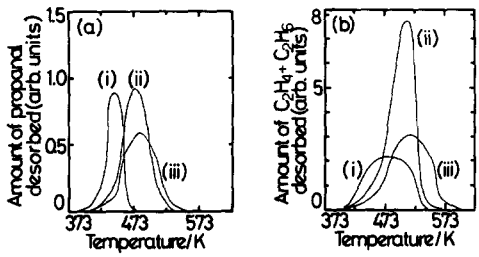

FIG. 11. TPD spectra of propanal (a) and ethene + ethane (b) from the surface species produced during ethene hydroformylation; TPD spectra were taken under conditions identical to those in Fig. 10 in the presence of H_2 (13.3 kPa).

acted with H_2 to desorb as propanal, while the propionate species was decomposed to form ethene and ethane in the presence of H_2. Almost the same amount of CO as ethene + ethane was also evolved at the same desorption temperature.

These results could be used in the determination of the amount of the surface species observed by FT–IR. The propanoyl and propionate species produced by ethene hydroformylation were desorbed and the peak intensities in the IR spectra correspond to the amounts of the products desorbed. The TPD experiment on the sample having only propionate species was also conducted to quantify the peak intensity of the propionate species observed by FT–IR. The reaction rates of the surface species in Table 4 were obtained on the basis of these quantitizations of the IR peaks.

Isotope Effects of $^{13}C^{18}O$ and D_2 on the Reaction Rates

In order for the effects of Se addition on each reaction step in the hydroformylation to be examined, $^{13}C^{18}O$ and D_2 instead of $^{12}C^{16}O$ and H_2, respectively, were employed. For Rh/ZrO_2, the rate of ethane formation on the Rh/ZrO_2 catalyst markedly decreased by replacing H_2 by D_2 as shown in Table 5. The isotope effect (v_D/v_H) was given to be 0.34. On the contrary, no isotope effect was observed for the formations of propanal and propanol. For the Se–Rh/ZrO_2 catalyst (**2**), the isotope effects were 0.63 (ethane), 0.50 (propanal), and 0.61 (propanol), showing similar values. The results using $^{13}C^{18}O$ are shown in Table 6. No isotope effect was observed for ethane formation on the Rh/ZrO_2 catalyst; however, the rate of the formations of propanal and propanol decreased to 0.82–0.84 by using $^{13}C^{18}O$ instead of $^{12}C^{16}O$. For the Se–Rh/ZrO_2 catalyst (**2**), no isotope effect was observed for the formations of all the products as shown in Table 6.

DISCUSSION

It was found that $(CH_3)_2Se$ can react with the surface OH groups and oxygen atoms on the ZrO_2 surface above 573 K, while in the presence of Rh particles (36 Å for 1 wt% and 45 Å for 3 wt%) on the ZrO_2 support, $(CH_3)_2Se$ selectively reacted with the hydrogen atoms preadsorbed on the Rh metal surface in the temperature range 373–573 K as shown in Fig. 1. The Se atoms thus deposited onto the Rh particles (catalysts (**1**)) were stable and were not lost during ethene hydroformylation at 453 K as shown in Fig. 2. The Se atoms supported by a coimpregnation method using aqueous solution of $Rh(NO_3)_3$ and SeO_2 behaved similarly to those derived from $(CH_3)_2Se$ in Fig. 2. Figure 4 exhibits the oxidation state of Se to be −2. Thus most of the Se in the catalysts (**2**) is distributed as dianions on the Rh metal surfaces because the Se atoms on the ZrO_2 surfaces would be situated in a positive oxidation state and/or at least show a different

TABLE 5

Isotope Effects of D_2 on the Rates for the Formations of Ethane, Propanal, and Propanol in Ethene Hydroformylation at 453 K

Catalyst	$v(D_2)/v(H_2)$		
	Ethane	Propanal	Propanol
Rh/ZrO_2	0.34	1.00	1.20
Se–Rh/ZrO_2(0.019)	0.63	0.50	0.61

Note. Rh, 1 wt%; C_2H_4:CO:H_2 (or D_2) = 13.3:8.0:8.0 kPa.

TABLE 6

Isotope Effects of $^{13}C^{18}O$ on the Rates for the Formations of Ethane, Propanal, and Propanol in Ethene Hydroformylation at 453 K

Catalyst	$v(^{13}C^{18}O)/v(^{12}C^{16}O)$		
	Ethane	Propanal	Propanol
Rh/ZrO_2	1.07	0.84	—
$Se-Rh/ZrO_2(0.019)$	1.03	0.93	0.98

Note. Rh, 1 wt%; C_2H_4: $^{12}C^{16}O$ (or $^{13}C^{18}O$): H_2 = 13.3 : 3.3 : 3.3 kPa.

XPS spectrum from that for the Se atoms on Rh metal and also because the H_2 adsorption vs Se content plots similar to that for the catalysts (**1**) were obtained as shown in Fig. 3. The amount of CO adsorbed did not largely reduce with an increase of Se content as compared with the H_2 adsorption. Particularly, CO could adsorb on the catalysts having the smaller Se contents as with the catalyst without Se. This is entirely different from the case of H_2. From the curve for H_2 adsorption in Fig. 3, one Se atom is supposed to block eight surface Rh atoms for H_2 adsorption on the catalysts (Rh 1 and 3 wt%). Figure 12 shows the Se atom adsorbed on the Rh(111) plane which is often exposed on Rh particles (*22*): Rh_A and Rh_B sites are 6 per Se atom and the sum of Rh_A, Rh_B, and Rh_C sites are 12 per Se atom. Unlike the block of Se to H_2 adsorption, Se may promote CO adsorption on Rh_B sites in a way similar to S adatoms (*23, 24*).

The promoting effects of Se additives on the hydroformylation of ethene on the catalysts (**1**) were found in Fig. 6. The large enhancement by Se was observed for propanol formation. Propanal was more preferably produced than propanol on the Rh/ZrO_2 catalyst, whereas on the $Se-Rh/ZrO_2$, propanol was a main product for the hydroformylation. The selectivity of hydroformylation showed a maximum value at Se/Rh = 0.66 which is more than four times larger than the selectivity for the Rh/ZrO_2 catalyst. The promotion of the hydroformylation rates by the optimum amount of Se added was also observed with the catalysts (**2**) (1 and 3 wt%) as shown in Figs. 7 and 8. The catalysts (**1**) prepared by using $(CH_3)_2Se$ more selectively produced propanal and propanol than the catalysts (**2**) obtained by the coimpregnation method. The difference of the promoting effects between the two types of catalysts is not clear, but the microscopic environments of Se at Rh metal surfaces may be somewhat different though the XPS spectra of Se 3*d* and Rh 3*d* levels for both catalysts were the same. In fact the amounts of added Se for the maximum selectivity are different between the catalysts (**1**) and (**2**). The common feature of both catalysts observed in IR spectra is the disappearance of the twin CO peaks by Se addition as shown in Fig. 9, suggesting the preferential deposition of Se on the twin sites which are often considered to be located on corner and step sites of Rh particles. Therefore, it is also supposed that the microscopic morphology of the Rh particles on ZrO_2 is different with the two catalysts and hence the different amounts of Se may be required to make the Se-modified surface selective for hydroformylation.

Konishi *et al.* (*25*) reported that S poisoned selectively Rh sites which might have been bridging-CO adsorption sites, and corner or edge sites (CO twin sites) were relatively less affected by S. They also demonstrated that the S poisoning reduced the

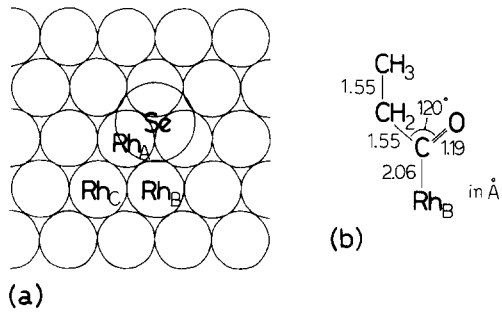

FIG. 12. (a) Three different Rh sites around Se on Rh(111) surface and (b) conformation of propanoyl species.

hydrogenation activity, leaving the hydroformylation activity on the twin sites without S blocking and the selectivity of hydroformylation was apparently enhanced. However, we do not have any definite evidence that S atoms introduced from H_2S preferentially adsorb on the bridge sites of Rh flat surface rather than on the corner or edge sites. Furthermore, Egawa and Iwasawa (*26*) have reported that S atoms formed by H_2S dissociative adsorption selectively poison the step sites of Ru(1,1,10) stepped surface and after the completion of the poisoning of step sites, S atoms possibly adsorb on the terrace of the stepped surface. This finding on Ru(1,1,10) coincides with the present IR observation on the Se–Rh/ZrO_2 catalysts. Pauling's electronegativities are almost the same for S and Se. The hydroformylation reaction rate per Rh bare site was enhanced about 10 times by Se addition and propanol formation was promoted more than 70 times as shown in Fig. 6, whereas the enhancement by S addition was only 1.8 times. The difference in atomic radius may be one of important factors (S^{2-}, 1.84 Å; Se^{2-}, 1.98 Å); i.e., Se can interact with CO or propanoyl on the far site (Rh_B) in Fig. 12a, but S may be not efficiently interact with C atoms for those species on far sites.

The peaks at 1776, 1770, and 1766 cm^{-1} for the catalysts (**2**) with Se/Rh = 0, 0.019, and 0.061, respectively, in Fig. 9 appeared only under reaction conditions, no peak around 1770 cm^{-1} being observed upon CO adsorption. The TPD spectra for propanal formation in the presence of H_2 agreed well with the behavior of these peaks for each catalyst as shown in Figs. 10 and 11. Furthermore, the peak was reproduced by propanal adsorption at 190 K in the presence of H_2, followed by heating under vacuum. The peak was converted to the propionate species contributed with asymmetric and symmetric O–C–O stretching vibrations as given in Tables 3 and 4. These results demonstrate that the peaks at 1766–1776 cm^{-1} are of propanoyl species.

The desorption temperature of the propanoyl species in Figs. 10 and 11 shifted to the higher temperatures by Se addition: 462 K for Rh/ZrO_2, 473 K for Se–Rh/ZrO_2 (0.019), and 486 K for Se–Rh/ZrO_2 (0.061). The carbonyl band of propanoyl species also shifted from 1776 to 1766 cm^{-1} as shown in Table 3. The peak intensity for propanoyl species on the Se–Rh/ZrO_2 catalyst which is most selective for hydroformylation was 2.7 times as large as that for the Rh/ZrO_2 catalyst. These results suggest that Se^{2-} interacts with the propanoyl species and also promotes its formation. As already mentioned, the theoretical study and the behavior observed in Fig. 3 suggest that Se^{2-} enhances CO adsorption on Rh_B sites in Fig. 12, where there may be a weak interaction between Se 4*p* and CO $2\pi^*$ levels. Thus, the ethyl migration to CO(ad) (CO insertion) may occur on the Rh_B sites assited by Se.

The structure of the propanoyl ligand coordinated on the Rh atom in $[Rh_6(CO)_{15}(COEt)]^-$ (*27*), which is regarded as a model structure for the propanoyl species on the Rh/ZrO_2 catalysts, is shown in Fig. 12b. When propanoyl adsorbs on the Rh_B site in Fig. 12a, the distance between Se and carbonyl carbon is estimated to be 3.18 Å. The Se–C bond length in $(CH_3)_2Se$ is 1.943 Å. Therefore, it is possible that the adsorption of propanoyl on the Rh_B atom geometrically has some interaction between Se and the carbonyl carbon. The stabilization of the propanoyl species by Se leads to preferable formation of propanol as shown in Figs. 5, 6, and 8. This is compatible with the promotion of the conversion from propionate to propanoyl by Se addition as shown in Table 4.

The reaction mechanism for ethene hydroformylation on the Se–Rh/ZrO_2 catalysts is shown in Fig. 13. No isotope effect in the formations of propanal and propanol on the Rh/ZrO_2 catalyst was observed with D_2 as shown in Table 5, but the isotope effects of $^{13}C^{18}O$ were observed on Table 6, suggesting that the rate-determining step for hydroformylation on the Rh/ZrO_2 catalyst is the CO insertion. On the contrary, on the

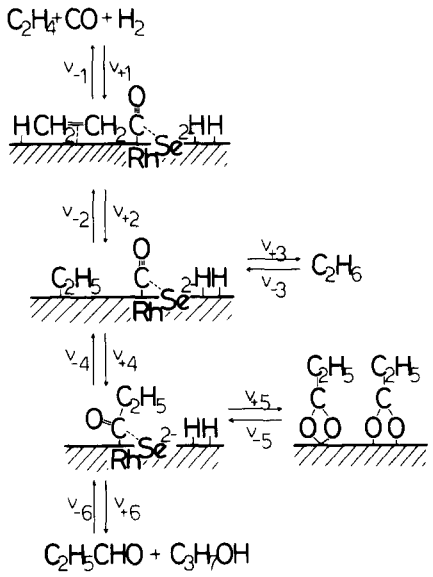

FIG. 13. Reaction mechanism for hydroformylation on the Se-modified Rh/ZrO_2 catalysts.

$Se–Rh/ZrO_2$ catalyst, the isotope effects for the formations of propanal and propanol were observed with D_2 and not with $^{13}C^{18}O$ as shown in Tables 5 and 6, suggesting that the CO insertion step is not rate-determining due to the assist by Se and rather that the dissociative adsorption of H_2 is suggested to be the slowest step. This may be also supported by the facts that the reaction rate for hydroformylation was proportional to the H_2 pressure. Thus, it is demonstrated that Se^{2-} on Rh assists CO adsorption and CO insertion, and as a result increases the concentration of the propanoyl intermediate of hydroformylation in the steady state, where the rate-determining step for the hydroformylation switched over from the CO insertion process on the Rh/ZrO_2 catalyst to theH_2 dissociation step on the $Se–Rh/ZrO_2$ catalysts.

CONCLUSIONS

(1) Se added to Rh/ZrO_2 promoted the hydroformylation reaction of ethene. The large enhancement of the rate (ca. 10 times in TOF for the formations of propanal and propanol) was observed particularly with the catalyst modified by $(CH_3)_2Se$, on which the formation of propanol rather than propanal was enhanced more than 70 times as compared with the propanol formation on the unmodified Rh/ZrO_2 catalyst.

(2) Se markedly increased the selectivity of hydroformylation. The dependency of the rate and selectivity upon the Se content showed the presence of an optimum Se quantity for hydroformylation.

(3) XPS revealed that Se and Rh are situated in the -2 and metallic states, respectively, where a direct Se–Rh bonding (2.41 Å for $Se–Rh/ZrO_2$ derived from $Rh_6(CO)_{16}/(CH_3)_2Se$) is suggested.

(4) Se^{2-} suppressed the adsorption of H_2 more drastically than that of CO, one Se atom blocking the 8 Rh sites for H_2 adsorption.

(5) The reaction intermediate, propanoyl species for ethene hydroformylation were observed with the largest amount on the catalyst having the optimum Se content.

(6) Se^{2-} is suggested to interact with CO and propanoyl adsorbed on the far site (Rh_B) in Fig. 12, which may enable the promotion of CO insertion step.

(7) These effects of added Se switched the rate-determining step from the CO insertion on the Rh/ZrO_2 catalyst to the dissociative adsorption of H_2 on the $Se–Rh/ZrO_2$ catalysts.

(8) Se may be superior to S as a promoter adatom for hydroformylation, Se being larger in size and softer than S.

REFERENCES

1. (a) Sachtler, W. M. H., and van Santen, R. A., *in* "Advances in Catalysis" (D. D. Eley, H. Pines, and P. B. Weisz, Eds.), Vol. 26, p. 69. Academic Press, New York, 1977; (b) Biswas, J., Bickle, G. M., Gray, P. G., Do, D. D., and Barbier, J., *Cat. Rev.* **30,** 161 (1988).
2. Lee, V. D., and Ponec, V., *Catal. Rev. Sci. Eng.* **29,** 183 (1987).
3. "Metal-Support and Metal-Additive Effects in Catalysis" (Imelik, Naccache, Coudurier, Praliaud, Meriaudeau, Gallezot, Martin, and Vedrine, Eds.). Elsevier, Amsterdam, 1982.
4. Goodman, D. W., *Acc.Chem. Res.* **17,** 194 (1984).

5. Naito, S., and Tanimoto, M., *J. Chem. Soc. Chem. Commun.*, 1403 (1989).
6. Wilson, T. P., Kasai, P. H., and Ellgen, P. C., *J. Catal.* **69,** 193 (1981).
7. Steveson, S. A., Lisitsyn, A., and Knözinger, H., *J. Phys. Chem.* **94,** 1576 (1990).
8. (a) Ichikawa, M., Hoffmann, P. E., and Fukuoka, A., *J. Chem. Soc. Chem. Commun.*, 1395 (1989); (b) Ichikawa, M., and Fukushima, T., *J. Phys. Chem.* **89,** 1564 (1985).
9. Bhasin, M. M., Bartley, W. J., Ellgen, P. C., and Wilson, T. P., *J. Catal.* **54,** 120 (1978).
10. (a) Ichikawa, M., Lang, A. J., Shriver, D. F., and Sachtler, W. M. H., *J. Amer. Chem. Soc.* **107,** 7216 (1985); (b) Jen, H. W., Zheng, Y., Shriver, D. F., and Sachtler, W. M. H., *J. Catal.* **116,** 361 (1989).
11. Levin, M. E., Williams, K. J., Salmeron, M., Bell, A. T., and Somorjai, G. A., *Surf. Sci.* **195,** 341 (1988).
12. (a) Underwood, R. P., and Bell, A. T., *J. Catal.* **109,** 61 (1988); (b) Underwood, R. P., and Bell, A. T., *J. Catal.* **111,** 325 (1988).
13. Kinennemann, A., Breault, R., Hindermann, J. P., and Laurin, M., *J. Chem. Soc. Faraday Trans. 1* **83,** 2119 (1987).
14. Nielsen, J. R. R., and Pederson, K., *J. Catal.* **59,** 395 (1979).
15. MacLaren, J. M., Vvedensky, D. D., Pendry, J. B., and Joyner, R. W., *J. Catal.* **110,** 243 (1988).
16. Feibelman, P. J., and Hamann, D. R., *Phys. Rev. Lett.* **52,** 61 (1984).
17. MacLaren, J. M., Pendry, J. B., and Joyner, R. W., *Surf. Sci.* **178,** 856 (1986).
18. Ogawa, A., Kondo, K., Murai, S., and Sonoda, N., *J. Chem. Soc. Chem. Commun.*, 1283 (1982).
19. Ogawa, A., Miyake, J., Karasaki, Y., Murai, S., and Sonoda, N., *J. Org. Chem.* **50,** 384 (1985).
20. Izumi, Y., Asakura, K., and Iwasawa, Y., *J. Chem. Soc. Chem. Commun.*, 1327 (1988).
21. Rochester, C. H., and Terrell, R. J., *J. Chem. Soc. Faraday Trans. 1* **73,** 596 (1977).
22. (a) Lyon, H. B., and Somorjai, G. A., *J. Chem. Phys.* **46,** 2539 (1967); (b) Belton, D. N., and Schmieg, S. J., *Surf. Sci.* **202,** 238 (1988).
23. Rewick, R. T., and Wise, H., *J. Phys. Chem.* **82,** 751 (1978).
24. "The Chemical Physics of Solid Surfaces and Heterogeneous Catalysis" (D. A. King, Ed.). Elsevier, Oxford, 1982.
25. Konishi, Y., Ichikawa, M., and Sachtler, W. M. H., *J. Phys. Chem.* **91,** 6286 (1987).
26. Egawa, C., and Iwasawa, Y., *Surf. Sci.* **198,** L329 (1988).
27. Ciani, G., Sironi, A., Chini, P., and Martinengo, S., *J. Organometall. Chem.* **213,** C37 (1981).